Received: 13 November 2025 | Revised: 24 April 2026 | Accepted: 24 April 2026

DOI: 10.1002/mp.70478

RESEARCH ARTICLE

MEDICAL PHYSICS

Impact of LET-modifying planning objectives on the optimization of mixed-modality proton–photon treatments

Lisa Seckler[1,2] | **Amit Ben Antony Bennan**[1,3] | **Niklas Wahl**[1,3]

[1]Division of Medical Physics in Radiation Oncology, German Cancer Research Center—DKFZ, Heidelberg, Germany

[2]University of Applied Sciences (THM), Giessen, Germany

[3]Heidelberg Institute for Radiation Oncology and National Center for Radiation Research in Oncology, Heidelberg, Germany

Correspondence
Lisa Seckler and Niklas Wahl, Division of Medical Physics in Radiation Oncology, German Cancer Research Center—DKFZ, Im Neuenheimer Feld 280, 69120 Heidelberg, Germany.
Email: lisa.seckler@dkfz-heidelberg.de and n.wahl@dkfz-heidelberg.de

Funding information
Deutsche Forschungsgemeinschaft, Grant/Award Number: 443188743

Abstract

Background: The linear energy transfer (LET) correlates with the relative biological effectiveness (RBE); thus, the increase of LET in depth in proton therapy leads to elevated RBE and a higher risk of toxicity in healthy tissue beyond the target. Jointly optimized combined proton–photon treatments may serve as a means to redistribute LET and avoid high-LET regions in organs at risk (OARs).
Purpose: To mitigate LET-related toxicity in OARs, this work leverages combined treatments by direct integration of LET in the joint optimization process. To this end, LET-modifying objective functions and variable RBE models are used within a joint optimization framework for combined proton–photon treatments. This approach combines the properties of both modalities to achieve LET-shaping and satisfy biological dose objectives in the target and OAR.
Methods: LET-modifying objective (LMO) functions based on the dose-weighted LET (LETxDose) and on *dirty dose*—defined as high-LET dose above a defined LET-threshold— were integrated into joint optimization within the open source toolkit *matRad* (v2.10.1). Treatment plans with phantom and clinical test cases were optimized and evaluated, consistently using the same dose objectives in each plan. The compared plans use the following: (1) constant RBE model, (2) variable RBE models, (3) *dirty dose* objectives, (4) LETxDose (LxD) objectives. Furthermore, sensitivity analysis was performed for various penalty weights, different proton beam angles and α–β ratios. The plans were assessed for target coverage, dose conformity, and LET reduction in OARs, combining five proton fractions with 25 photon fractions.
Results: LET-modifying objectives enabled localized reduction of high-LET exposition in OARs by redistributing dose contributions of both modalities. Protons provided superior tumor-targeted dose delivery and reduced integral dose, while photons mitigated high-LET at the distal edge without compromising dose conformity in the tumor. Beam alignment had a greater influence on enhancing the LMO effect than the number of proton beams. The *dirty dose* to 2% of brain stem volume was reduced when using joint LET optimization approaches. LET-modifying squared underdosing objectives increased the *dirty dose* in the GTV by up to 102% compared with the reference joint plan, whereas squared overdosing objectives reduced the *dirty dose* in the brain stem by 96%. Their combination achieved a 94% increase of *dirty dose* in the GTV with a corresponding reduction in the brain stem. Despite 2 Gy per fraction, the proton-only plan resulted with a 7.5 times higher *dirty dose* per fraction in a joint optimized plan using *dirty dose* objectives, approximately 5 Gy locally per fraction. Using LETxDose

objectives, it was 3.3 times higher. *Dirty dose* objectives provided more explicit LET control than LETxDose, with minimal compromise in target coverage.
Conclusion: Integrating LET-based objectives into a jointly optimized proton–photon system allows for direct steering of the combined LET, improving dose conformity and reducing high-LET exposure in critical regions. This approach leverages modality-specific strengths and offers a practical route toward LET-optimized multimodality radiotherapy for safer, more effective treatments.

KEYWORDS
combined treatments, *dirty dose*, LET-modifying joint optimization, spare OAR

1 | INTRODUCTION

In a proton beam, the linear energy transfer (LET) increases with depth and is highest at the distal edge of the Bragg peak. Although clinical guidelines apply a constant radiobiological effectiveness (RBE) of 1.1 to convert the absorbed physical dose into a biologically equivalent photon dose, evidence shows that RBE increases with LET.[1–3] Accounting for the increased differential biological effectiveness is advantageous for enhancing tumor control at the target site. However, this elevated effectiveness is potentially detrimental when high-LET regions extend into surrounding, target-adjacent organs at risk (OARs).[4,5] Moreover, the biological effectiveness of protons at the end-of-range remains uncertain, as no consensus exists on the appropriate RBE in these regions, leading to uncertainties in the predicted RBE within OAR.[6]

These uncertainties in RBE modeling suggest the direct integration of LET into treatment plan optimization as a surrogate for RBE estimation.[7–9] Grün et al.[10] demonstrated that the dose-averaged LET can serve as a reliable predictor of RBE, particularly in regions with a narrow LET spectrum. The integration of LET-based objectives in conjunction with RBE-weighted optimization has also been proposed as a strategy to reduce interpatient variability in the biological effectiveness of proton treatment plans.[6,7,11–14] Additionally, optimization approaches have been introduced to explicitly steer the placement of proton track-ends away from critical structures.[15] Within the target volume, LET-based treatment planning has been explored through LET painting techniques, aiming to enhance tumor control probabilities in radio-resistant, hypoxic tumors.[16,17]

In parallel to the developments in LET painting strategies, joint optimization approaches were proposed to exploit biological properties of different modalities[17–25] and better usage of limited availability of proton slots.[26] These approaches differ in complexity of the applied biological models depending on the modalities combined. Still, they utilize an RBE-weighted dose[17–25] or biological effect formulation for their optimization problem, only indirectly steering LET. In this context, LET is decisive for the biological effect of radiation on tissue and should be considered directly. The aforementioned studies provide convincing arguments for combined radiation planning, an approach that enables direct LET steering in order to shift the RBE correlated LET to correspond to the individual treatment plan.

This work proposed to apply the recent developments in proton LET painting to the joint optimization approach combining existing photon therapy resources and proton therapy resources, guided by LET-modifying objectives, that can address the limitations of proton-only LET-based optimization regarding the need of multiple beam configurations.[27] For instance, LET-based objectives within the target volume can lead to increased integral dose due to higher entrance doses and reduced conformity of the high-dose region,[4] which cannot be compensated for by protons alone, using standard clinical techniques.[27] Combined proton–photon planning allows existing technology to be easily used to directly control LET distributions. The combined mixed-modality approach presented in here employs combined simultaneous optimization of photon beamlet and proton spot intensities in order to deliver the prescribed cumulative dose, with each treatment fraction assigned to a single modality.[18–24]

In this study, jointly optimized mixed-modality proton–photon treatment plans are employed to the following:

1. Systematically compare the approaches of LET-weighted dose optimization, *dirty dose*[28] optimization, and variable RBE-based optimization strategies for mitigating elevated end-of-range biological effects in target-adjacent OAR, and
2. demonstrate the potential of mixed-modality planning to achieve more homogeneous distributions of LET-weighted dose and *dirty dose* within the target volume.

This metric is based on the premise that biological damage is more likely for the high-LET component of the absorbed dose. *Dirty dose* refers to the component of dose delivered by particles with LET values exceeding a predefined threshold. Both approaches use LET-based

objectives, which are collectively henceforth referred to as LET-modifying objectives (LMOs).

2 | METHODS AND MATERIALS

2.1 | Joint optimization problem

This work is based on joint optimization of the total effect of photon and proton contributions.[18,19] The total effect ϵ is accumulated as the sum of the effect of each photon and proton fraction $\epsilon = n_\gamma(\alpha d + \beta d^2)$, derived from the given survival fraction $S = e^{-\alpha d - \beta d^2}$ based on the linear-quadratic (LQ) model.[25,29] This formulation enables consistent accumulation of heterogeneous fraction doses within the framework of the LQ model. The corresponding optimization problem can be stated as follows:

$$\begin{aligned}
\underset{w}{\text{minimize}} \quad & \mathcal{F}(w) = \sum_m p_m \, f_m(\varepsilon^{\text{Total}}(w)) \\
\text{subject to} \quad & \varepsilon_i^{\text{Total}} = n^\gamma \varepsilon_i^\gamma + n^P \varepsilon_i^P && \forall i \\
& \varepsilon_i^\gamma = \alpha_i^\gamma \sum_j D_{ij}^\gamma \, w_j^\gamma + \beta_i^\gamma \left(\sum_j D_{ij}^\gamma \, w_j^\gamma \right)^2 && \forall i \\
& \varepsilon_i^P = \sum_k \alpha_{ik}^P D_{ik}^P \, w_k^P + \left(\sum_k \sqrt{\beta_{ik}^P} D_{ik}^P \, w_k^P \right)^2 && \forall i \\
& w_j^\gamma \geq 0 && \forall j \\
& w_k^P \geq 0 && \forall k
\end{aligned} \tag{1}$$

The objective function $\mathcal{F}(w)$, composed of weighted individual objectives $f_m(\varepsilon^{Total}(w))$, each representing a planning goal and scaled by a penalty parameter p_m. The total biological effect in voxel i, denoted ε^{Total}, is calculated as the sum of photon ε_i^γ and proton ε_i^P fraction biological effects, each multiplied by their respective number of fractions, n^γ and n^P.

The intensity of a given photon beamlet j is represented by w_j^γ, with the dose contribution to voxel i per unit intensity defined by the dose influence matrix D_{ij}^γ. Similarly, w_k^P denotes the intensity of proton spot, and its corresponding physical dose contribution to voxel i is represented by D_{ik}^P. The LQ model coefficients α_i^γ and β_i^γ represent reference photon parameters, while the effective proton LQ coefficients, α_{ik}^P and β_{ik}^P, vary spatially along the path of proton beamlet k.

Under the assumption of a constant RBE for proton therapy, effective α and β values were equated to the photon parameters, and the proton dose was scaled by a factor of 1.1. The optimization process solved for the set of photon beamlet (w_j^γ) and proton spot (w_k^P) intensities that result in an optimal spatial distribution of the total biological effect.

This study evaluates objective functions (f_m) based on both biological effect and LET-dependent metrics, specifically *dirty dose* and LET-weighted dose (LETxDose).

2.2 | Introducing LET-modifying objectives

For the purpose of this work, two LET-painting strategies were found of interest. The first approach optimized on dose-weighted LET. The second approach utilized the concept of *dirty dose*, which was recently introduced to have a dose-like metric indicating high-LET regions.[28] LET was reported as dose-averaged LET (*LETd*), and as such also used when computing variable RBE-models. *LETd* was employed, which accounts for energy straggling and the production of secondary particles during beam-medium interactions and is the most commonly used definition of LET for RBE models.[1,13] The LET spectrum was approximated using precomputed look-up tables based on Monte Carlo simulations available within matRad for all available energies of protons. This model assumed a simplistic constant lateral LET for steps in depth. The LET contribution matrix LET_{ij} was used for all LMOs.[13]

2.2.1 | LET-weighted dose (LETxDose)

LETxDose is defined as the LET scaled by absorbed dose. For computational efficiency, the LET-weighted dose contributions were stored in a matrix (L_{ij}):

$$L_{ij} = LET_{ij} \cdot D_{ij} \tag{2}$$

Here L_{ij} is the LET-weighted dose contribution of beamlet j in voxel i resulting from the LET matrix LET_{ij} and the dose influence matrix D_{ij}.

Unlike dose, LET is a radiation-specific characteristic and cannot be offset against the number of fractions. To approximate total LET value, a treatment-averaged LET was computed, termed quasi-*LETd*, by averaging over dose:

$$LETd_i^{\text{quasi}} = \frac{n^\gamma L_{ij}^\gamma \cdot w_j^\gamma + n^P L_{ij}^P w_j^P}{n^\gamma D_{ij}^\gamma \cdot w_j^\gamma + n^P D_{ij}^P w_j^P} \tag{3}$$

where additional the index P denotes the particle therapy modality component, while the index γ defines the photon component. The variable n stands for the number of fractions of the respective beam type, while w defines the intensity of the given beamlet. LET quantities have a positive correlation to biological effect. Typical LET optimized cases look at a constant LET

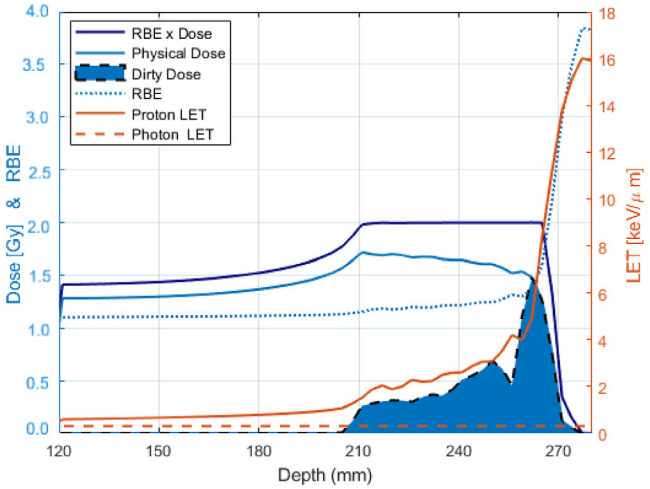

FIGURE 1 *Dirty dose* component (LET threshold = 2 keV/μm) of physical dose in a spread out Bragg peak optimized with the McNamara variable RBE model. Also shown on the axis on the right, dose averaged LET of protons and the constant LET assumed for photon beams.

value over all fractions; however, in our case, LET varies over fractions and there exists no way to sum them or biologically interpret a summation. Therefore, the quasi *LETd* offered a simple accumulation of varying LET over various fractions.

2.2.2 | Dirty dose (DD)

Dirty dose (DD) is the component of the physical dose delivered by high-LET (*LETd*) areas of a proton beamlet, as visualized in Figure 1. The *DD* concept is from Heuchel et al.,[28] the *DD* used here depends solely on an LET-threshold. The *dirty dose* influence matrix (D^{Dirty}) can be written mathematically as follows:

$$D_{ij}^{\text{Dirty}} = \begin{cases} D_{ij} & \text{for } LET_{ij} > k^{Dirty} \\ 0 & \text{else} \end{cases} \quad (4)$$

in which D_{ij}^{Dirty} describes the *dirty dose* contribution for each voxel i from pencil beam j. D_{ij}^{Dirty} was obtained by applying a threshold to the LET contribution matrix LET_{ij} and sampling the dose contributions D_{ij} for voxel–pencil beam (i, j) pairs with LET contributions greater than the LET threshold k^{Dirty}.

2.3 | Treatment planning

2.3.1 | AAPM TG119 phantom case

Initial testing and sensitivity analysis for the LET objectives were investigated for the AAPM TG119[30] phantom. The proton and photon combinations were optimized on the physical dose optimization. Standard objective functions were used for this purpose. These include squared deviation (SD), squared overdosing (SO), and the mean dose (MD) objective. While SD aims to achieve the reference value and is therefore mostly used for tumor regions, SO seeks to achieve the minimum value, making it a popular choice for OAR. MD was used to reduce the integral dose in the body. For the TG119 phantom, three different kinds of plans optimized on physical dose were observed as follows:

1. Reference jointly optimized plan (proton and photon), only using dose objectives.
2. Joint + DD plans using dose objectives and additional different *dirty dose* objectives in the OAR.
3. Joint + LET plans using dose objectives and additional different LETxDose (LxD) objectives in the OAR.

TABLE 1 Basic dose objectives (SD or SO) of the structures of the AAPM TG119 phantom, target, body and OAR, that remain the same for each treatment plan for the initial test and the sensitivity analysis. In addition, a MD objective is added as a secondary objective for the body in order to control the integrated dose of the protons to the surrounding tissue (body). The first number in parentheses represents the penalty, while the second number reflects the prescribed dose.

Structure	Dose objective [Gy]
Target	SD(800,60)
OAR	SO(100,30)
Body	SO(100,30)
	MD(100,0)

All plans used a constant RBE of 1.1 and a dose grid resolution of 3 mm. The objective settings for the sensitivity analysis are shown in Table 1. Additional *dirty dose* and LETxDose objectives with a prescribed dose of 0 Gy were added to the joint optimized plans using different penalty weightings (DD: 10, 30, 100, 300 and LxD: 6, 10, 30, 100) to provide a qualitative evaluation of the objective function's behavior. Nine equidistant photon beams and three proton beams were employed.

Additionally, to study the impact of number of proton beams, three different proton beam angle settings ((0°), (−45°, 45°) and (−45°, 0°, 45°)) for the joint + DD plan were also investigated. The LMOs penalty weight was kept fixed at 100.

The dose objectives remained the same for each plan, while LMOs varied with each plan. Both *dirty dose* and LETxDose objectives were applied to OARs and are described in more detail in Figures 2 and 3. The difference in unit dimensionality between LETxDose and *dirty dose* was taken into account by applying an additional objective penalty of 6 keV Gy μm^{-1} for LETxDose, as the physical dose affects the objectives. The objective penalty weight of 6 keV Gy μm^{-1} was

determined by dividing the standard penalty factor of 100 by the squared proton LET of 4 keV μm^{-1} at the Bragg peak (i.e., $100/4^2 = 6.25$), which was rounded to the nearest integer.

The open-source treatment planning platform *matRad* (v2.10.1)[31–33] was used to implement joint optimization of combined treatments and LET-based optimization objectives.[19,25] The optimization problem was solved using the interior point optimizer (IPOPT).[34]

2.3.2 | Clinical case

Following initial validation using the TG119 phantom, the developed methods were applied to a clinically relevant case, an anaplastic astrocytoma patient from the glioma image segmentation dataset (GLIS-RT).[35] This patient case was selected due to the proximity of the gross tumor volume (GTV) to the brain stem, a scenario where LET-based modulation could be particularly beneficial. The GTV was treated as a boost volume with an integrated boost strategy.

Five fractions of intensity-modulated proton therapy (IMPT) delivered at 265° and 285°, and 25 fractions of photon-intensity-modulated radiotherapy (IMRT) using nine equidistant coplanar beams were considered. The number of fractions assigned to each modality was predefined, rather than optimized, and was selected based on clinical precedent for boost treatments.[36] The fraction allocation decision was made based on a clinical trial of particle therapy boost treatments for glioblastoma.[36]

The following treatment plans were generated and compared:

1. Proton-only plan using a constant RBE model, representing standard clinical practice and the lower limit on dose conformity and LET shaping.
2. Jointly optimized reference plan (Ref Joint) using the McNamara variable RBE model for protons,[2] this establishes the baseline impact of joint optimization and upper limit on dose shaping and conformity.
3. Joint + LMOs for OAR comparing *dirty dose* objectives and LET-weighted dose objectives for OAR.
4. Joint + LMOs for OAR comparing *dirty dose* objectives and LET-weighted dose objectives for target.
5. Joint + DD or LET plan incorporating MinMax objectives.
7. Each plan (1–5) again with a different α–β ratio

The dose grid resolution for optimization was 5 mm in all directions. The energy range for proton beams spanned 31.729 – 236.107 MeV, while photons were modeled using a clinically standard 6 MV energy.

In addition, a photon-only plan was incorporated into the comparison in order to demonstrate the advantages of the modalities and mixed planning, as shown in Table 7. The photon plan also used the objectives mentioned in Table 2 and applied 30 fractions.

TABLE 2 Primary treatment planning objectives for physical dose (same for all plans) and for the reference proton-only plan. SD was used for the tumor structures and SO was used for the healthy tissue. Additionally, a MD objective was added to the body.

Structure	Objectives	Penalty	Prescribed dose [Gy]
CTV	SD	800	60
GTV	SD	1000	68
Brain stem	SO	100	50
Chiasm	SO	200	30
Body	SO	100	30
	MD	100	0

TABLE 3 LMOs as SO objectives that were added to the treatment plans, joint-optimized *dirty dose*, and L × D plan, in the brain stem, as well as a MD objective that was added to the brain stem in the reference (Ref) joint-optimized plan. Also, LMOs as SU objectives were added for the GTV in separate treatment plans.

Plan type	OAR	Objectives	Penalty	Prescribed dose [Gy]
Ref joint	Brain stem	MD	100	0
DD joint	Brain stem	DD SO	100	0
LET joint	Brain stem	LxD SO	100	20
DD joint	GTV	DD SU	100	18
LET joint	GTV	LxD SU	100	90

In order to maintain the readability of the plans and reduce the number of variables for the analysis in this work, no fractionation benefit was assumed ($\alpha/\beta_{Healthy} \geq \alpha/\beta_{Tumor}$). Photon LQ model parameters were set to $\alpha = 0.1\,Gy^{-1}$ and $\beta = 0.05\,Gy^{-2}$ for both tumor and healthy tissue. Conversely, the clinical case was intended to represent actual clinical situations, and therefore $\alpha/\beta_{Healthy} \leq \alpha/\beta_{Tumor}$ must also be considered. 6 Gy was an assumed average value of Grades 3 and 4 of malignant glioma from the in vitro data in Table 2 from Qi et al.[37] Therefore, an α value of $0.25\,Gy^{-1}$ and a β value of $0.0417\,Gy^{-2}$ were specified for the GTV and CTV.[38–40]

Dose objectives for the reference plan are listed in Table 2. SD objectives were applied to the tumor volumes, SO objectives to OARs, and a MD objective to the body to limit integral dose.[31,32] This reference plan contained standard objectives that remained in every plan (Table 2). No additional biological dose constraints were imposed.

LMOs were integrated depending on the plan type. SO objectives were used for OARs and squared underdosing (SU) objectives were applied in the GTV (Table 3).

$$f^{\text{LMO sq overdosage}} = \frac{1}{N_S} \cdot \sum_{i \in S} \Theta(q_i(LET_i, d_i) - q^{ref}(LET_i, d_i)) \cdot (q^{ref}(LET_i, d_i) - q_i(LET_i, d_i))^2 \quad (5)$$

$$f^{\text{LMO sq underdosage}} = \frac{1}{N_S} \cdot \sum_{i \in S} \Theta(q^{ref}(LET_i, d_i) - q_i(LET_i, d_i)) \cdot (q^{ref}(LET_i, d_i) - q_i(LET_i, d_i))^2 \quad (6)$$

where $q_i(LET_i, d_i)$ is the LET-modifying quantity in voxel i. For *dirty dose*, $q_i(LET_i, d_i) = D_{ij}^{\text{Dirty}} w_j$ and for LET-weighted dose $q_i(LET_i, d_i) = L_{ij} w_j$. N_S describes the number of voxels in the structure and q^{ref} the prescribed dose.

A *dirty dose* threshold of 2 keV/μm was used, consistent with the suggested range for protons (1–4 keV/μm).[28] A value of 2 keV μm^{-1} was selected as it corresponds to a point on the rising slope, at approximately 66% of the maximum dose, of an individual proton Bragg peak. This approach ensured adequate tumor coverage while enabling the preferred extraction of dose based on high-LET contributions from the surrounding healthy tissue. For photons, a constant LET value of 0.3 keV/μm was assumed, representing secondary electrons interactions.[41]

3 | RESULTS

3.1 | Sensitivity analysis with the TG119 phantom

To assess the contribution of each modality, proton and photon, and the impact of LMOs, cumulative dose distributions (over all fractions) and LET metrics were compared across plans. Figure 2 presents reference and LET-modifying plans, including those with *dirty dose* objectives applied to a standard core and an extended region (core-big).

According to the reference plan for the joint treatment, the majority of the target dose is delivered by the three proton beams, with photons contributing merely a minor portion. The incorporation of *dirty dose* objectives to reduce high-LET exposure in the OAR shifts the modality balance, resulting in an increased photon dose contribution in the vicinity of the OAR, as shown in Figure 2. This effect becomes more pronounced with increasing penalty weighting, yielding a progressively higher photon contribution in these regions.

A comparison is also made for additional plans with LETxDose objectives, seen in Figure 3. The cumulative physical dose is compared over the different plans.

Similar to the application of *dirty dose* objectives, the usage of LETxDose objectives leads to an increased photon dose fraction. In contrast to the *dirty dose* approach, however, the effect of LETxDose objectives is already pronounced at low penalty weights and yields a more pronounced reduction of the high LET dose in the vicinity of the OAR.

3.1.1 | Analysis of the impacts on LET-modifying objectives for a different number of proton beams

In order to verify the influence of the proton angles on the strength of the LMOs, after verifying the impact of different penalty weights in Figures 2 and 3, the plans for one, two, and three proton beams were analyzed. The joint reference plan as well as the joint *dirty dose* plan and the joint LETxDose plans with prescribed dose of 0 Gy and a penalty of 100 are compared for the total physical dose in Table 4 and for the total *dirty dose* in Table 5.

While the prescribed target dose remains almost constant, the physical dose delivered to healthy tissue increases. However, no clear correlation with the number of proton beams can be observed. Furthermore, the *dirty dose* in healthy tissue decreases substantially, accompanied by a slight increase within the target area.

A comparison of a single proton beam (0°) with three beams (−45°, 0°, 45°) demonstrates a more pronounced reduction in *dirty dose* when using three beams, whereas the effect is less pronounced with two beams (−45°, 45°), indicating a dependence on beam arrangement.

For all beam configurations, the LETxDose objective provides greater sparing of the OAR (core) compared to the *dirty dose* objective, both in terms of physical dose and *dirty dose*. This improved sparing comes at the cost of increased dose delivery to surrounding healthy tissue and a partial reduction in target coverage.

3.2 | LET-modifying objectives in the OAR for the clinical case

3.2.1 | Reference plans

The proton-only plan for the clinical case delivers a uniform dose of 2 Gy to the CTV and 2.26 Gy to the GTV with an integrated boost. As expected, it results in the lowest MD to surrounding tissue due to the absence of photon contributions.

In contrast, the reference jointly optimized plan delivers the majority of the dose through five proton fractions, while the photon fractions are used to enhance dose conformity and reduce the dose contribution from the proton entrance channel. The improvement in dose

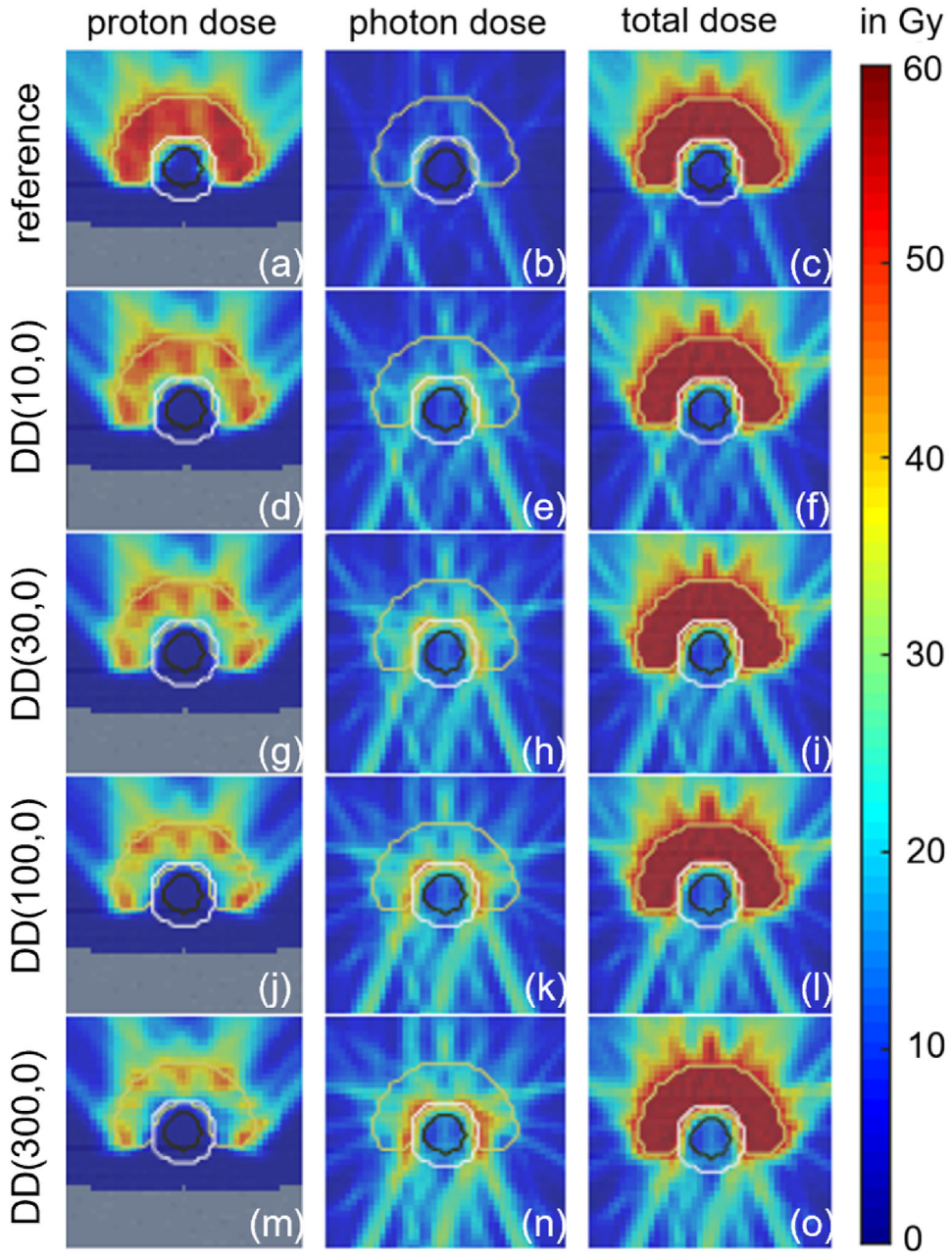

FIGURE 2 Comparison of proton and photon physical dose contribution to the total dose considering *dirty dose* SO objectives with varied penalty and constant prescribed *dirty dose* of 0 Gy with regard to the reference plan. The dose objectives applied are listed in Table 1.

conformity enabled by the additional degrees of freedom in the joint optimization is reflected in the reduced near-maximum dose in the brain stem ($BED_{2\%}$), as shown in Table 6.

3.2.2 | LET-modifying jointly optimized plans

All plans yield comparable target dose coverage, as illustrated by the cumulative BED–volume histograms in Figure 4.

In the jointly optimized plans that incorporate LMOs, the interface between the CTV and the brain stem receives increased photons dose. At this interface region, both proton and photon contributions are of similar magnitude, delivering approximately 2 Gy per fraction. The cumulative $BED_{2\%}$ in the brain stem for both LMO plans is similar to that observed in the proton-only plan. However, due to the increased reliance on photons, the LMO-based plans appear to trade LET reduction for a higher MD in the brain stem.

The *dirty dose* to 2% of the brain stem volume ($D_{2\%}^{\text{Dirty}}$) accumulated over 30 fractions is substantially higher in

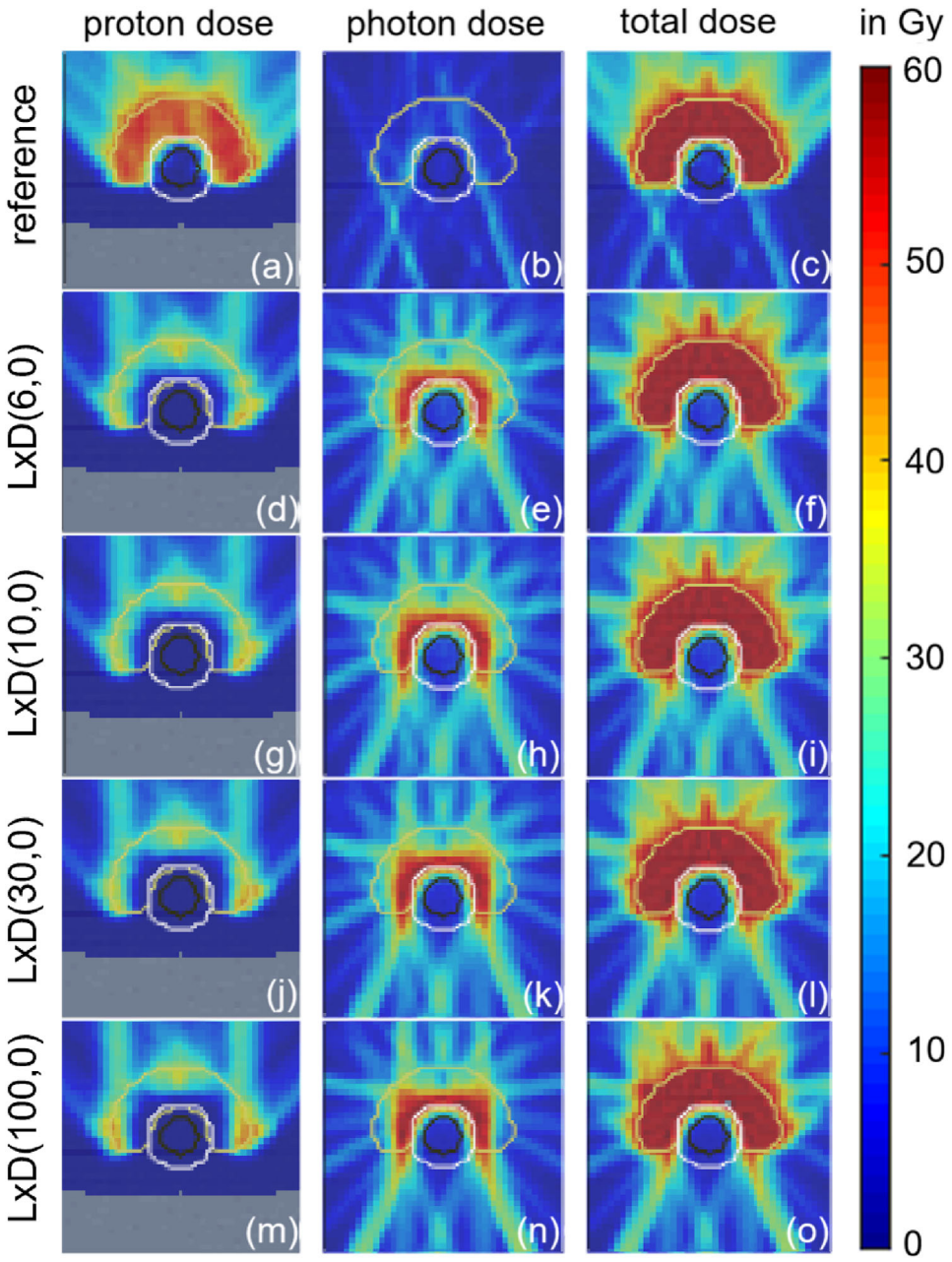

FIGURE 3 Comparison of proton and photon physical dose contribution to the total dose considering L × D SO objectives with varied penalty and constant prescribed L × D of 0 Gy with regard to the reference plan. The dose objectives applied are listed in Table 1.

the proton-only plan compared to the Joint + DD and Joint + LET plans (both computed over five fractions). Although the proton-only plan delivers 2 Gy per fraction and the LMO joint plans deliver approximately 5 Gy to the target, one might initially expect the proton-only plan to yield a lower *dirty dose*. However, the per-fraction *dirty dose* in the proton-only plan exceeds that of the Joint + DD and Joint + LET plans by factors of 7.5 and 3.3, respectively. These results suggest a clear benefit of incorporating LMOs. An overview of cumulative BED and dirty BED quality metrics for all plans is provided in Table 6. Dirty BED refers to the biologically effective dose (BED) resulting from the *dirty dose* component of the dose.

Figure 5 compares the joint treatment plans per fraction for the clinical case incorporating LMOs for OARs with the reference plans (proton-only and reference joint), as defined in Table 3.

The observed contributions of the photon and proton doses are consistent with the LMO behavior identified in the sensitivity analyses using the TG119 phantom. In the proton-only plan, the proton dose fraction is reduced and

TABLE 4 Comparison of the total physical dose between the reference joint plan, joint + DD (100,0), and joint + LET (100,0) for three different numbers of proton beams (1, 2, and 3) for the TG119 phantom's different structures. Each stated dose is in gray.

			Physical dose [Gy]				
Number of beams	**Plan**	**Structure**	**Mean**	**Max**	**Min**	D_5	D_{95}
	Reference	Core	5.12	16.36	1.01	9.39	1.38
		Target	59.79	63.00	44.82	61.40	57.51
		Body	3.28	63.00	0.00	21.27	0.00
1	DD(100,0)	Core	11.56	21.66	2.49	17.85	3.21
		Target	59.76	63.29	45.71	61.40	56.95
		Body	4.22	63.29	0.00	27.10	0.00
	LxD(100,0)	Core	6.55	13.04	2.31	11.23	3.03
		Target	59.68	64.04	43.79	61.89	56.93
		Body	4.09	64.04	0.00	27.57	0.00
	Reference	Core	7.97	24.71	0.97	15.19	1.46
		Target	59.81	63.70	42.90	61.36	57.54
		Body	3.46	63.70	0.00	26.25	0.00
2	DD(100,0)	Core	12.03	21.79	2.15	17.56	2.86
		Target	59.78	63.21	45.84	61.50	57.37
		Body	4.01	63.96	0.00	24.55	0.00
	LxD(100,0)	Core	7.11	13.81	2.60	11.88	3.35
		Target	59.67	63.89	44.26	61.82	56.68
		Body	4.60	63.89	0.00	28.80	0.00
	Reference	Core	5.88	21.86	0.62	14.09	0.98
		Target	59.82	63.28	41.42	61.18	57.97
		Body	3.13	63.28	0.00	23.02	0.00
3	DD(100,0)	Core	11.06	18.87	1.96	16.50	2.66
		Target	59.79	62.98	45.50	61.41	57.54
		Body	3.87	62.98	0.00	24.26	0.00
	LxD(100,0)	Core	6.47	12.82	2.27	11.12	2.97
		Target	59.69	63.81	44.33	61.89	56.87
		Body	4.20	63.81	0.00	27.55	0.00

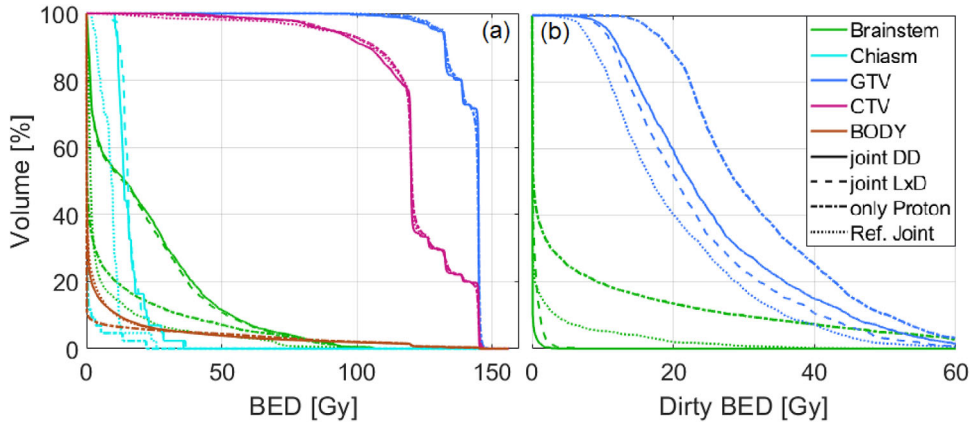

FIGURE 4 Modified dose–volume histograms for plans with LMOs (joint DD and joint LxD), as well as the proton-only plan and the reference joint plan. Squared overdosing objectives for OAR in a (a) BED–volume histogram and a (b) *dirty dose*–volume histogram for the brain stem.

TABLE 5 Comparison of the total *dirty dose* between the reference joint plan, joint + DD (100,0), and joint + LET (100,0) for three different numbers of proton beams (1, 2, and 3) for the TG119 phantom's different structures. Each stated dose is in gray.

			Dirty dose [Gy]				
Number of beams	**Plan**	**Structure**	**Mean**	**Max**	**Min**	D_5	D_{95}
	Reference	Core	1.34	10.88	0.00	5.15	0.00
		Target	19.85	50.50	0.26	44.18	3.29
		Body	0.43	50.50	0.00	0.00	0.00
1	DD(100,0)	Core	0.03	0.40	0.00	0.16	0.00
		Target	12.57	38.17	1.13	26.14	3.47
		Body	0.27	38.17	0.00	0.00	0.00
	LxD(100,0)	Core	0.00	0.00	0.00	0.00	0.00
		Target	10.55	46.46	0.00	29.33	0.13
		Body	0.25	46.46	0.00	0.00	0.00
	Reference	Core	2.85	19.59	0.00	9.73	0.14
		Target	24.00	56.03	6.53	41.63	11.43
		Body	0.49	56.03	0.00	0.00	0.00
2	DD(100,0)	Core	0.13	1.64	0.00	0.60	0.00
		Target	15.74	49.28	1.76	29.97	4.58
		Body	0.34	49.28	0.00	0.00	0.00
	LxD(100,0)	Core	0.00	0.00	0.00	0.00	0.00
		Target	7.98	32.98	0.00	19.58	0.07
		Body	0.22	40.68	0.00	0.00	0.00
	Reference	Core	2.69	18.95	0.00	10.40	0.08
		Target	26.32	57.78	5.20	49.90	10.10
		Body	0.55	57.78	0.00	0.00	0.00
3	DD(100,0)	Core	0.12	1.54	0.00	0.54	0.00
		Target	17.87	49.44	1.97	32.51	5.64
		Body	0.38	49.44	0.00	0.01	0.00
	LxD(100,0)	Core	0.00	0.00	0.00	0.00	0.00
		Target	11.67	48.02	0.00	31.85	0.13
		Body	0.28	48.02	0.00	0.00	0.00

TABLE 6 Table of treatment plan quality indicators based on cumulative BED and cumulative *dirty dose* for plans with LMO applied to OAR (brain stem). Each value is given in gray.

Cumulative BED [Gy]	**Only proton**	**Reference Jointly Opt.**	**Jointly Opt. DD**	**Jointly Opt. LxD**
GTV $D_{95\%}$	131.3	131.9	129.6	129.7
CTV $D_{95\%}$	96.3	97.6	94.6	94.4
Brain stem $D_{2\%}$	83.9	69.4	87.8	85.8
Brain stem mean	9.5	6.8	21.3	20.6
Body mean	2.7	3.8	3.6	3.5
Cumulative dirty BED [Gy]				
Brain stem mean	7.6	1.6	0.1	0.4
Brain stem $D_{2\%}$	62.4	19.9	0.9	2.3
Brain stem std. dev.	15.9	5.2	0.3	0.7
GTV mean	32.4	20.2	72.2	23.4
GTV $D_{2\%}$	64.7	47.9	95.7	54.1
GTV std. dev.	12.4	11.1	16.9	11.6

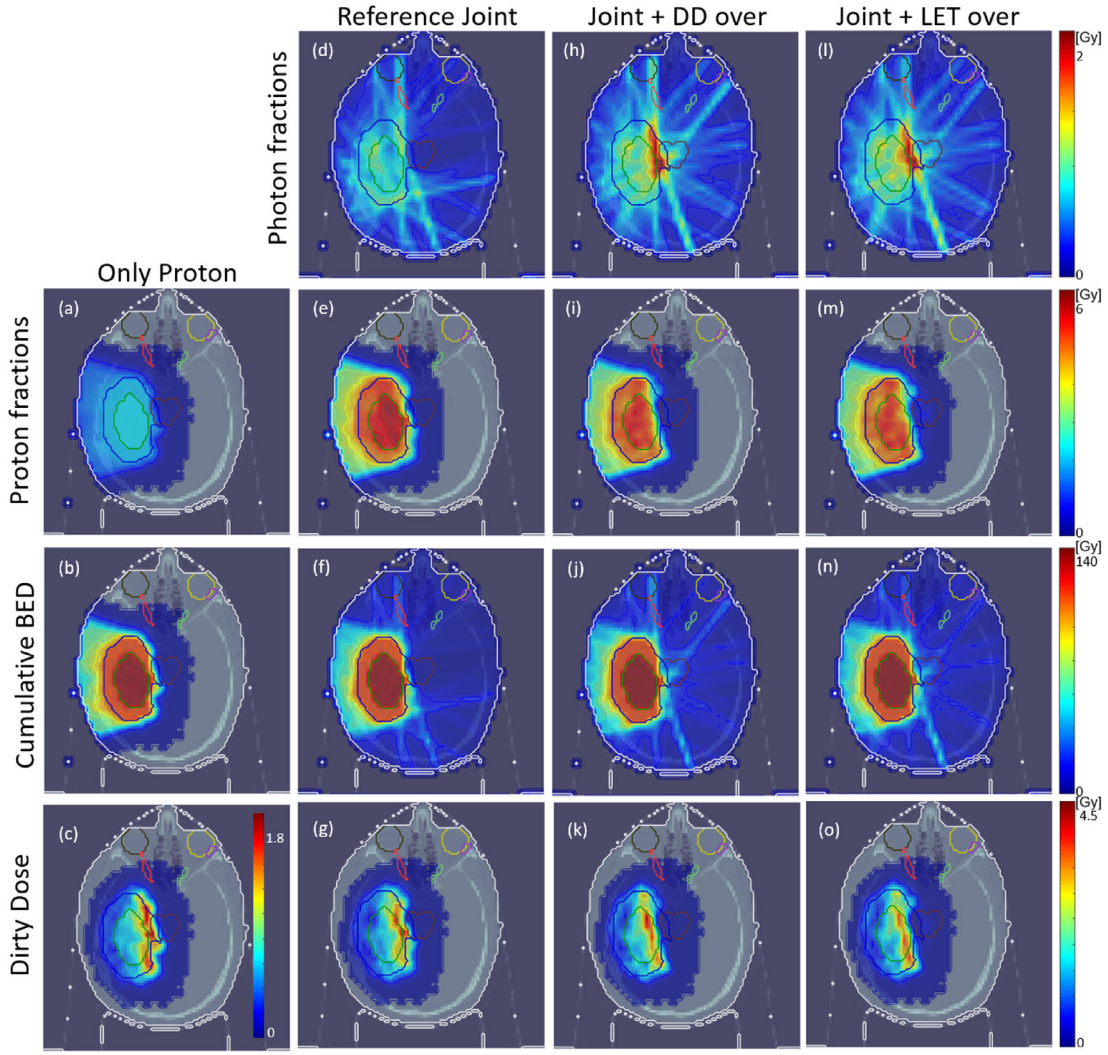

FIGURE 5 Visualized photon fractions (d, h, l), proton fractions (a, e, i, m), cumulative BED (b, f, j, n) and *dirty dose* (c, g, k, o) for a proton-only plan (a–c), a reference jointly optimized plan (d–g), a joint plan with a DD overdosing objective (h–k), and a jointly optimized plan with an LET overdosing objective (l–o). *Dirty dose* shown here is also dependent on the fraction dose, hence the proton-only plan (2 Gy per fraction) has an adjusted color scale for *dirty dose* seen in subfigure (c).

dirty dose is lower compared to the reference joint optimized plan, resulting in an increased cumulative BED along the beam entry path.

3.3 | LET-modifying objectives in the target for the clinical case

As in the previous analysis, these plans are compared to a 30-fraction proton-only treatment and a basic jointly optimized proton–photon plan (Figure 5). The resulting plans integrating LMOs for the GTV are presented in Figure 6, visualizing the photon and proton fractions. In these cases, the proton dose is concentrated at the proximal side of the GTV. The associated dose fall-off across the target leads to elevated LET in the GTV, but also results in cold spots, regions with insufficient dose. Photon dose is used to compensate for under-irradiated regions where protons are not contributing.

Although the proton-only plan exhibits a higher cumulative near-maximum dose in the GTV, the plans incorporating LMOs demonstrate reduced variability in high-LET dose within the target. Notably, the Joint + DD SU plan achieves a higher mean *dirty dose*, while the Joint + LET plan yields the lowest *dirty dose* values, as the LETxDose objective does not explicitly suppress the high-LET component of the dose distribution.

The cumulative dosimetric quality indicators for these plans are summarized in Table 7.

All plans for achieving high-LET in the GTV yield comparable target dose coverage but more pronounced doses in healthy tissue, as illustrated by the cumulative BED–volume histograms in Figure 7.

TABLE 7 Table of treatment plan quality indicators based on cumulative BED and cumulative *dirty dose* for plans with LMO applied to the target (GTV). Each value is given in gray. Additionally, a comparison between the different plans and an only photon plan is made.

Cumulative BED [Gy]	Only proton	Only photon	Reference Jointly Opt.	Jointly Opt. DD	Jointly Opt. LxD
GTV $D_{95\%}$	131.3	132.1	132.0	131.9	132.2
CTV $D_{95\%}$	96.3	95.2	97.6	102.0	98.5
Brain stem $D_{2\%}$	83.9	96.2	69.4	94.1	93.6
Brain stem mean	9.5	38.4	6.8	21.1	31.5
Body mean	2.7	8.5	3.8	4.2	5.2
Cumulative dirty BED [Gy]					
Brain stem mean	7.6	0.0	1.6	0.2	1.1
Brain stem $D_{2\%}$	62.4	0.0	19.9	3.1	6.1
Brain stem std. dev.	15.9	0.0	5.2	1.2	1.7
GTV mean	32.4	0.0	20.2	40.9	18.6
GTV $D_{2\%}$	64.7	0.0	47.9	52.4	27.9
GTV std. dev.	12.4	0.0	11.1	7.7	3.8

TABLE 8 Table of treatment plan quality indicators based on cumulative BED and cumulative *dirty dose* for plans with LMO (MinMax: SO in OAR and SU in target) applied to the target and the brain stem. Each value is given in gray.

		Contribution			Contribution	
Cumulative BED [Gy]	MinMax DD	Proton	Photon	MinMax LxD	Proton	Photon
GTV $D_{95\%}$	131.5	—	—	129.8	—	—
CTV $D_{95\%}$	103.6	—	—	95.8	—	—
GTV mean	143.1	111.0	32.0	141.6	78.9	62.7
Brain stem $D_{2\%}$	94.2	—	—	92.5	—	—
Brain stem mean	24.0	0.3	23.6	25.0	0.3	24.6
Body mean	4.4	2.0	2.4	4.1	1.5	2.6
Cumulative Dirty BED [Gy]						
GTV mean	39.1	39.1	0.0	23.8	23.8	0.0
GTV $D_{2\%}$	53.8	—	—	46.5	—	—
GTV std.dev	8.3	8.3	0.0	8.3	8.3	0.0
Brain stem Mean	0.1	0.1	0.0	0.1	0.1	0.0
Brain stem $D_{2\%}$	1.3	—	—	1.1	—	—
Brain stem std.dev.	0.4	0.4	0.0	0.4	0.4	0.0

3.4 | Combined LET-modifying objectives

In order to highlight the effect of combining both LMOs in OAR (SO) and target (SU) for each joint plan, the dose–volume histogram is also considered (Figure 8) using these combined plans. The standard objectives from Table 2 are retained. The extent to which the combined plan differs from the pure application to the target is also addressed in the dose–volume histogram. While Figure 8a,b shows the different plans in terms of *dirty dose* in the brain stem and the GTV, Figure 8c,d focuses on the LETxDose. The comparison is made to analyze the combined objective planning using MinMax objectives in brain stem and GTV (Table 8). In order to compare the contributions of protons and photons, the $D_{95\%}$ values for the GTV as well as the $D_{2\%}$ for the brain stem must be omitted from Table 8, as no accurate contributions can be derived therefrom.

Figure 4 shows that the proton-only treatment plan has the highest dirty BED values, while all LMOs consistently reduce the dirty BED in the brain stem. In Figure 8, the combination plans (MinMax) also lead to increased BED for the GTV and CTV. A specific behavior can be observed with regard to dirty BED: The combination plans with *dirty dose* optimizations show higher dirty BED compared to LETxDose optimized plans. In contrast, the MinMax-DD joint plan presents a lower dirty BED as the joint DD SU plan, while the LETxDose MinMax combination plan produces a higher dirty BED compared to the joint LET SU plan in the target.

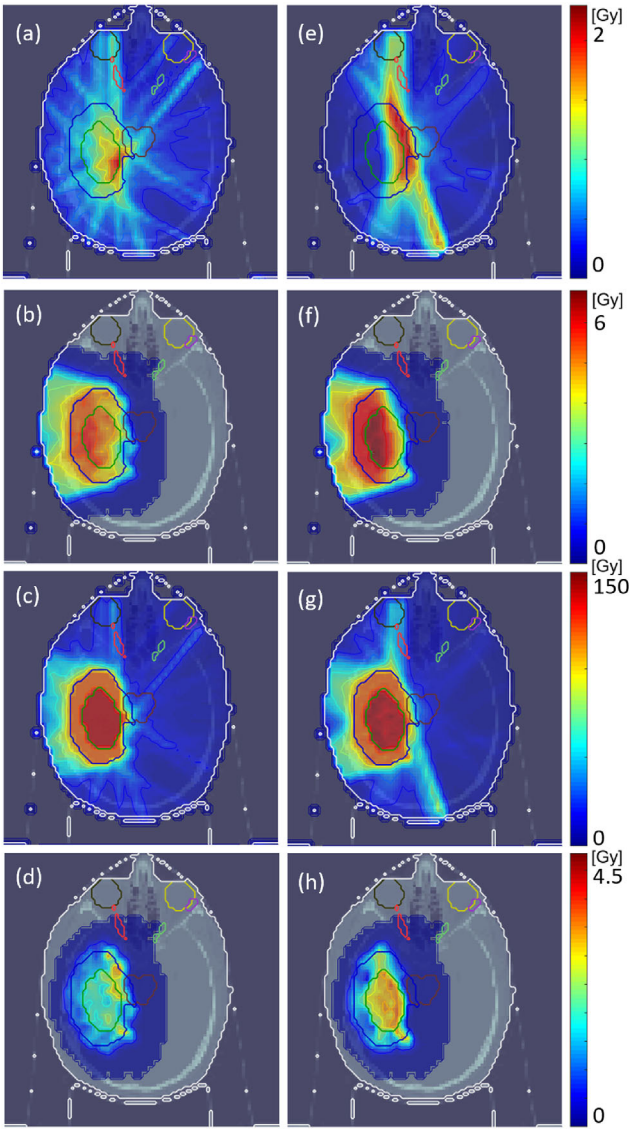

FIGURE 6 Visualized photon fractions (a, e), proton fractions (b, f), cumulative BED (c, g), and *dirty dose* (d, h) for a jointly optimized plan with a DD underdosing objective (a–d) and a jointly optimized plan with a LETxDose underdosing objective (e–h).

3.5 | Clinical $\alpha - \beta$ ratio

As representative of intracranial tumors, the α–β ratio for the tumor was assumed as 6 Gy instead of 2 Gy, while 2 Gy remains for the OAR.

Similar to the previous analyses, the plans (joint + DD and joint + LET) are compared with a 30-fraction proton-only treatment and a jointly optimized proton–photon plan (Figure 9). In these cases, the proton dose is concentrated on the proximal side of the GTV in order to reduce the high-LET doses in the brainstem. By using a higher α–β ratio in the tumor, the fractionation effect is taken into account. This allows the *dirty dose* to be reduced more sharply. The photon dose is used to compensate for under-irradiated areas where protons do not contribute and receives a larger proportion compared to an α–β ratio that is the same between the tumor and OAR.

To highlight the effect of combining both LET-modifying targets in OAR (SO) and target (SU) for each joint plan, the dose–volume histogram (Figure 10) using these combined plans is also considered. The standard objectives from Table 2 are retained. While Figure 10a,b shows the different plans in terms of *dirty dose* in the brainstem and GTV, Figure 10c,d focuses on LETxDose.

4 | DISCUSSION

This study is not intended as a quantitative comparison of optimization strategies on a case-by-case basis. Instead, it seeks to introduce and characterize the behavior of LMOs in the context of combined proton–photon therapy. The quadratic property of the LMOs and the associated trade-off between LET modulation and physical dose distribution lead to a variety of possible behaviors depending on the penalty and prescription of LET and *dirty dose*.

This study investigates the implementation of LET-based objectives (LMOs) for both OAR and the target volume within a jointly optimized mixed proton-photon treatment framework. For this purpose, a phantom and a patient case were examined. Two reference plans were evaluated: (1) a proton-only plan with an integrated boost, representing current state-of-the-art proton therapy; and (2) a jointly optimized proton–photon plan, representing an idealized mixed-modality scenario unconstrained by modality-specific planning limitations. In the jointly optimized plan, the MD objective applied to the body promotes a proton-dominant solution to minimize the integral dose. Photon beamlets are primarily employed to enhance dose conformity and reduce dose contributions in the proton entrance channel, leveraging the additional degrees of freedom provided by dual-modality planning.

4.1 | Requirements for comparison

Initial simplified comparisons on the TG119 phantom are based on physical dose and meant only to study the impact of LMOs on the tradeoffs between physical dose and LET. However, the heterogeneity of fraction doses achieved by joint optimization cannot be trivially summed up. Hence, the LQ model is used to sum the biological effects of individual fractions. Here, however, the proton versus photon dose contributions are affected by the α–β ratios of the target and surrounding tissue. This makes it difficult to ascertain the source of shown local tradeoffs of being from differential fractionation or from LMOs. In order to compare the various plans, the complex biological implications of differential fractionation were initially avoided. A simplifying assumption

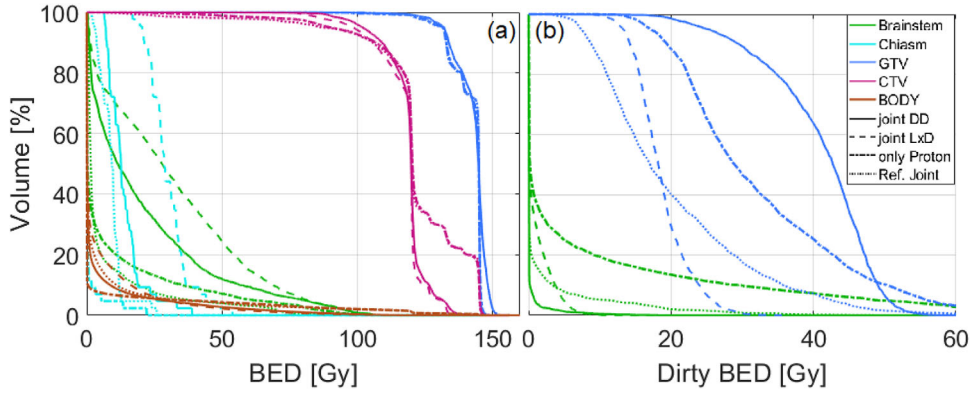

FIGURE 7 Modified dose–volume histograms for plans with LMOs (joint DD and joint LxD), as well as the proton-only plan and the reference joint plan. SU objectives for the target in a (a) BED–volume histogram and a (b) *dirty dose*–volume histogram for the GTV.

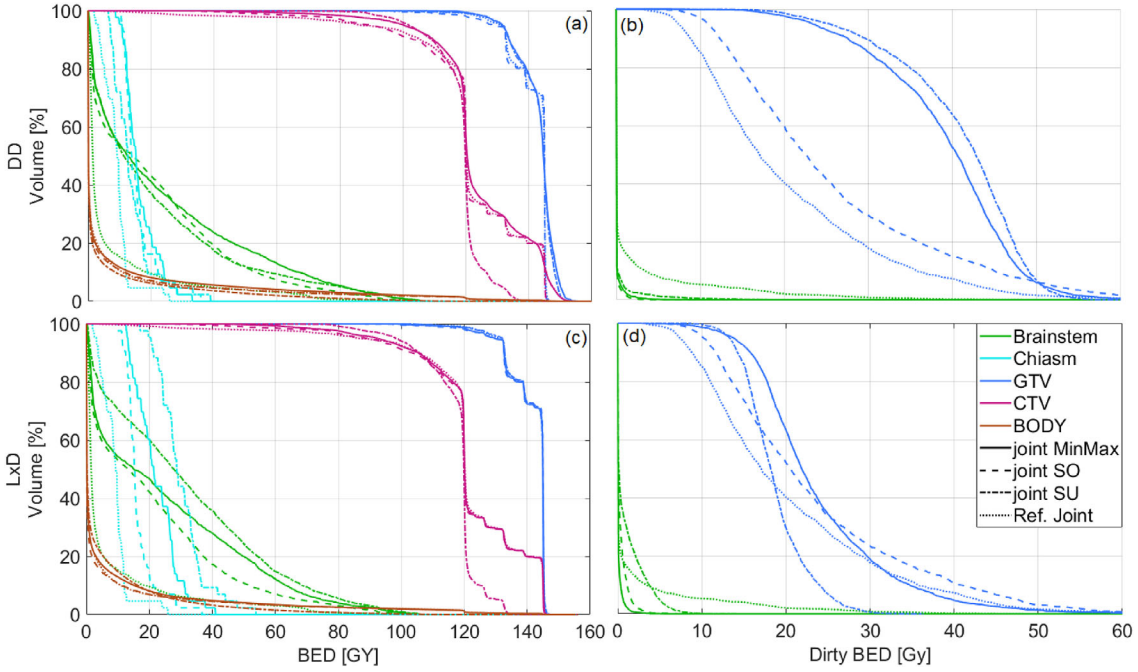

FIGURE 8 Modified dose–volume histograms (a, c), BED–volume histogram (b), (d) *dirty dose*–BED–volume histogram for plans based on LMOs: (a, b) DD and (c, d) LxD for OAR (SO) and the target (SU) as well as the combination (MinMax), comparing joint optimized plans to the reference joint plan.

was made: $\alpha/\beta_{Target} <= \alpha/\beta_{NormalTissue}$. This prevents photons from being preferentially assigned to subvolumes within the target, particularly near critical structure interfaces such as the brain stem.[18,19,22] Although, no discernible fractionation effect may be observed, photon irradiation continues to have a substantial role in shaping the physical dose distribution by improving dose conformity and to make-up for the trade-offs made in proton fractions. When there exists a fractionation benefit ($\alpha/\beta_{Target} > \alpha/\beta_{NormalTissue}$), the optimizer has the incentive to distribute fraction doses equally over all fractions (both photon and proton fractions). This increased photon contribution at all regions at the interface between the target and normal tissue. Since photon usage is often confined to small volumes at the end of range of the particle therapy beams, this strategy may be especially suitable for implementation in stereotactic and radiosurgical workflows to improve dose conformity. Photon contribution can be modulated via adjustment of the objectives strength or prescribed LET-based dose levels. The contribution of photon dose to cumulative dose distributions is influenced directly by the penalty applied to the LMOs.

In addition, uniform or high LET must be achieved within the target volume, which poses a considerable challenge, especially in the case of large or complex

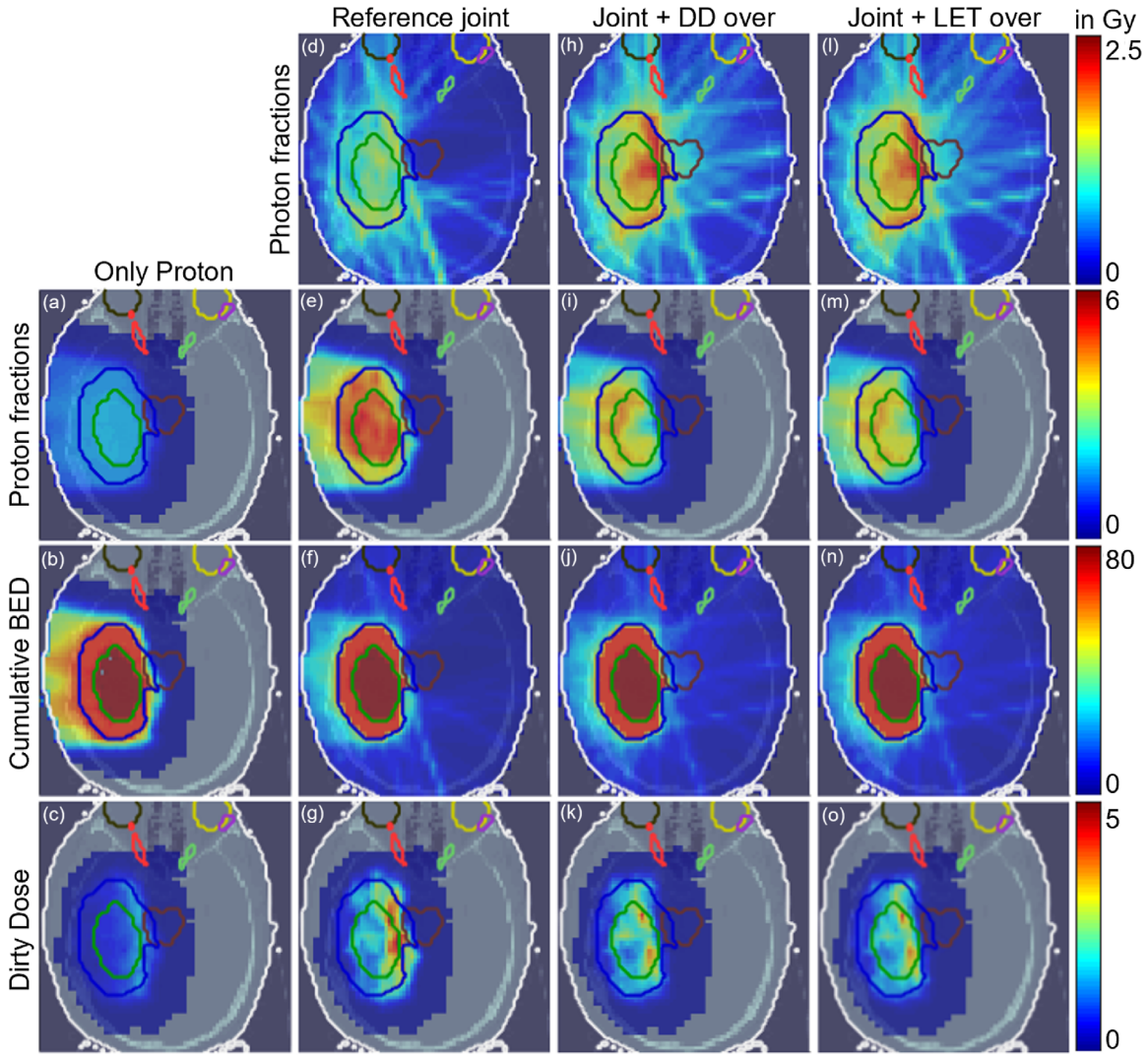

FIGURE 9 Visualized photon fractions (d, h, l), proton fractions (a, e, i, m), cumulative BED (b, f, j, n), and *dirty dose* (c, g, k, o) for a proton-only plan (a–c), a reference jointly optimized plan (d–g), a joint plan with a DD overdosing objective (h–k), and a jointly optimized plan with a LET overdosing objective (l–o). *Dirty dose* is shown as fraction dose, delivered from protons only. The color scales are in gray.

tumor geometries. To address this, multi-ion treatments, which combine ion beams of different qualities within a single treatment fraction, have been investigated as a means to enhance LET distributions in the target.[17,42] These approaches exploit the distinct radiation qualities and LET characteristics of different ion species, providing increased flexibility in shaping the intratumoral LET distribution. The concept of a "quasi" *LETd* is an artificial quantity to approximate a total LET value (Equation 3). However, it enables the accumulation and averaging of LET values over multiple heterogeneous fractionation schemes, providing a convenient strategy to compare treatments. It should also be noted that the current implementation approximates LET as a single average value per voxel, rather than modeling its full energy-dependent spectrum. While this simplification leads to approximation errors, this error is expected to be small and acceptable for current purposes due to the absence of a fragmentation tail in proton beams.

4.2 | Sensitivity analysis with the TG119 phantom

The sensitivity analysis with the TG119 phantom also shows clear differences in dose distribution when using the two LMOs. Figures 2 and 3 illustrate a redistribution of dose contribution between protons and photons, while maintaining consistent target coverage. As the LET-modifying objective penalty increases, photon involvement rises and proton contribution decreases, reflecting the reduction of undesirable proton *dirty dose* in the OAR situated beyond the target. This

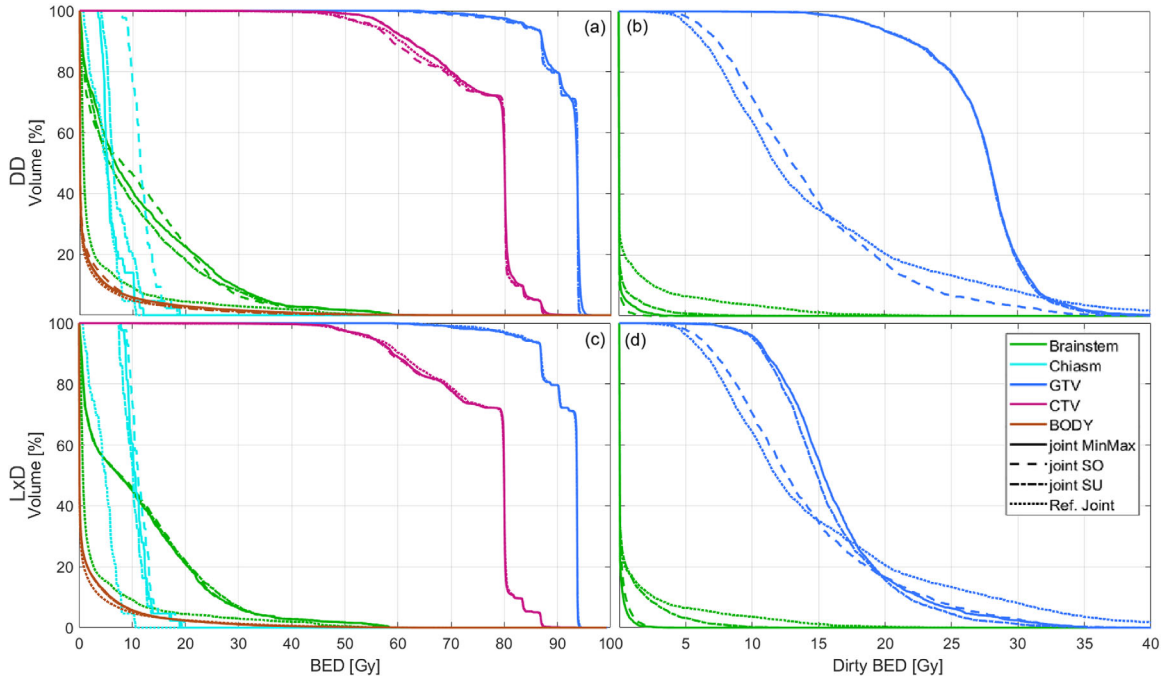

FIGURE 10 Modified dose–volume histograms for $\alpha/\beta = 6$ Gy : (a, c) BED–volume histogram, (b, d) *dirty dose*–BED–volume histogram for plans based on LMOs: (a, b) DD and (c, d) LxD for OAR (SO) and the target (SU) as well as the combination (MinMax), comparing joint optimized plans to the reference joint plan.

results in strategic LET redistribution that spares healthy tissue while maintaining target coverage. High-LET dose is effectively replaced by lower-LET dose coming from photons. The sharp-edged distributions of the physical dose of protons, using LETxDose, shown in Figure 3, are due to the nature of the *LETd* tables used in this study that average LET over every step of depth.

The selection of proton beam angles critically influences the outcome and effectiveness of LMOs. By increasing the number of proton beams and arranging for the distal falloff of the beam to be in close proximity to an OAR, the ability of these objectives to reduce the dose contributions associated with increased LET within the organ is improved.

Photon contribution in joint optimization is also influenced by beam angle selection, primarily for proton beams, due to their spatially variable LET. Beam angles whose distal edge does not terminate near OARs are less affected by LET-based objectives, suggesting that beam configuration remains a critical planning consideration.

4.3 | Analysis of LET-modifying objectives

When LMOs are introduced in the OARs, photons are employed to displace high-LET regions produced by proton beams near the brain stem in the patient case. Both *dirty dose*-based and LETxDose-based objectives appear to be similarly effective in this role, with photon dose substituting for high-LET proton dose in regions near critical structures as the brain stem.

Compared to the reference plans, both LMOs show a big drop in *dirty dose* delivered to the brain stem. The *dirty dose* SO plan and the LETxDose SO plan show a 99 % and 95.4 % decrease in cumulative *dirty dose* as compared to the clinical standard proton-only plan. This is achieved by using photons at the distal end of the proton beam located at the interface between the target and the brain stem, which reduces the *dirty dose* in the brain stem by approximately 6 Gy. However, the cost of this dramatic change is the increased MD in the brain stem and surrounding tissue from the photon fractions and a decrease of $D_{95\%}$ in the GTV by around 1.7 %, reflecting the redistribution of dose to spare the OAR. As presented in Table 7, the intensity modulated only photon treatment plan (IMRT) attains target coverage similar to that of the proton-only plan but at the cost of elevated doses to the brain stem and adjacent normal tissue. The integration of both modalities enables highly conformal target irradiation while minimizing the dose delivered to OAR, as evidenced by the reference jointly optimized plan.

The LETxDose prescription of 90 Gy keV/μm, which was used for underdose objectives in the GTV, also shows substantial differences to the reference plans and was based on the assumption that half of the prescribed target dose (30 Gy) would be delivered with an LET of

approximately 3 Gy keV/μm, which corresponds to the values observed at the Bragg peak. The underdosing objectives in Table 7 reveal pronounced differences in *dirty dose* application in the GTV. The cumulative dirty BED in particular indicates that the *dirty dose* in the GTV is 31% for joint optimization with *dirty dose* objectives, whereas only 24% is applied for the proton-only plan. Furthermore, this was achieved with a lower standard deviation in the cumulative dirty BED within the target. Naturally, such gains come at the cost of increased low-LET dose in the OARs and surrounding tissue. This low dose comes from photons used to maintain dose homogeneity and from the increase dose in proton entrance channels, related to LET painting. The reference jointly optimized plan shows the best achievable conformity and highlights the impact of the LMO on conformity. Joint DD exhibits superior optimization efficiency over joint LETxDose, primarily because the dose-weighting term in LETxDose limits the extent of LET-induced dose redistribution and reduction due to its dose component that must be taken into account.

In order to exploit the properties of SO and SU optimization to spare OAR and achieve maximum tumor damage, the combination of both objectives was investigated. The MinMax plans shown in Figure 8 and Table 8 utilize both minimum (SU) and maximum (SO) dose objectives. In addition, the proton and photon contributions were considered, which clearly show that the proton contribution, which has the higher biological effectiveness, predominates in the tumor, while the photon-dose contribution in the OAR is substantially higher. This effect is hardly noticeable in the tumor region when using LETxDose, as the photon contribution, due to the stronger shift in LET, has a greater impact as compared to *dirty dose* objectives. However, an assessment of the doses within a specific volume must be considered as a combined unit, as the dose distribution within the tissue volume is inseparably linked and a division into different modalities would not yield meaningful results.

Here the *dirty dose* MinMax plan shows plan quality indicators that are quite close to those of the individual *dirty dose* SU and *dirty dose* SO plans, which indicates that, though there are some trade-offs, there are sufficient degrees of freedom to almost achieve the cumulative results of the individual objectives. The *dirty dose* objectives behave quite predictably in the target and OAR. In this case, the minimum dose and maximum dose objectives compete as the GTV is in close proximity to the brain stem, in cases with more spatial separation, the objectives would be more easily achieved as the objectives would not compete for the same voxels. MinMax plans using LETxDose objectives, as mentioned before, do not produce as desirable results in the target. The further introduction of the SO objective to this increases the standard deviation of *dirty dose* in the target. Within the brain stem, the MinMax LETxDose plan does achieve similar *dirty dose* distribution as that seen for the individual SO LETxDose plan.

Finally looking at the plan using clinical α-β ratios, shown in Figure 9, clear increase in photon contribution is observed that stems from the optimizers incentive to apply photons to target-surrounding tissue interfaces. This behavior is in line with that seen for SO LMOs and does not compete. With regard to the target, however, the SU LMO and differential fractionation would be in competition. In the case shown above, the conflict is most seen at regions where the CTV and GTV delineations are closer in proximity dues to anatomical constraints.

4.4 | Objectives challenges

In addition, the *dirty dose* objective guarantees a minimal LET threshold of 2 Gy keV/μm within the GTV. This highlights that *dirty dose* may provide a more pragmatic approach to LET-based and biologically inspired treatment optimization. Currently, the chosen LET threshold (2 Gy keV/μm) for classifying *dirty dose* is a conservative choice within the range stated in earlier studies.[28] A more biologically justified threshold could be identified through retrospective analyses that correlate treatment outcomes or toxicities with LET distributions.[43–45] Ultimately, this could point to location-specific thresholds that are optimized for clinical relevance.

Initially, when optimization is performed solely in the proton-only plan and reference joint optimized plan without LET objectives, substantial fluctuations in *dirty dose* are observed in the target (GTV), as shown in Figure 5c,g. However, when LMOs are added, a more uniform distribution of the *dirty dose* within the GTV is observed. This suggests that LMOs can serve as effective instruments for ensuring a consistent baseline for the high-LET dose in the target area. Such uniformity could theoretically decrease the risk of local recurrence by maintaining a minimal biological effect that is not achievable with current RBE models. LETxDose objectives are of limited applicability, especially in larger target volumes because their nonspecificity allows the optimizer to satisfy the objective by delivering an additional dose from low-LET protons, which may compromise both the integral dose delivered in the entrance channel and the LET in the target. LETxDose objectives, however, did reduce variance in the delivered *LETd* in the target.

Observing the objectives, the quantification of objective strength is not trivial and cannot be converted into comparable penalties or a biologically equivalent metric, which complicates standardization across studies. The influence of an LMO depends strongly on its relative penalty strength, exact formulation and potential normalization of the corresponding objective functions.

4.5 | LET-modifying objectives evaluation

The results of this study show that combining both optimization strategies has a reinforcing effect on the distribution of the *dirty dose* with regard to either objective. However, this advantage is accompanied by an increased dose to the OAR, which is due to the additional contribution of photons. In comparison, biologically optimized plans based solely on variable RBE do not suppress the high-LET dose contributions in OARs as effectively. The reference jointly optimized plan also shows upper limit of the ability of a variable RBE model to spare healthy tissues as its usage of protons is to reduce integral dose in surrounding tissue and photons to improve conformity. Here it can be inferred that a proton-only plan using a variable RBE model would lie in the region between the two reference plans. The redistribution, when using LMOs in a joint plan, enhances the SU effect and underscores the strong correlation between physical and biological optimization parameters. In comparison, this effect is inverted when *dirty dose* optimization is performed, as no direct physical dose component is included in the optimization. Additionally, the inclusion of SO in the OAR indicates a secondary redistribution of the *dirty dose*, reducing its contribution in the adjacent GTV. These results demonstrate that the optimization method significantly influences not only the distribution of the BED but also the trade-off between target coverage and the preservation of the surrounding normal tissue. Since high-LET radiation increases the probability of complex DNA damage, limiting LET deposition in sensitive tissues such as the brain stem could reduce the risk of toxicity, even if the local physical dose is controlled and results in an increased average dose in healthy tissue. This is a trade-off that must be evaluated by clinicians to safely utilize this tool.

This irradiation strategy represents a clinically relevant advancement of conventional dose-based planning by incorporating a biological dimension. This approach offers the potential not only to improve tumor control, but also to reduce toxicity risks, address RBE-related uncertainties, and facilitate the exploration of more advanced modality-based treatment strategies.

For anatomically complex or high-risk regions in particular, LET-based optimization enables the deliberate redistribution of high-LET to target volumes where improved biological efficacy is desired, while sparing OAR.

4.6 | Outlook

Larger and more varied examinations, as well as standardized objective formulations are required to better quantify and benchmark these in this study examined effects. The flexibility of mixed-modality treatment optimization offers a unique platform to investigate these trade-offs without sacrificing target coverage.

Combined treatments with heterogeneous dose distributions, as proposed here, may be more susceptible to deterioration in plan quality from range and setup uncertainties. While this is less problematic for intracranial targets, as in the case of anaplastic astrocytoma studied here, robust optimization strategies will be indispensable for wider clinical applications.[21] A robustness analysis is provided in the supplementary material for the plans shown in this work. Figure 11 describes the robustness analysis for the TG119 phantom, while Figure 12 examines the clinical case. From a mono-modal treatment planning perspective, a larger number of proton beams offer more degrees of freedom in shaping the dose and LET, reducing the impact of a potential photon component.[46] Proton arc therapy, for example, facilitates LET painting.[47,48] Alternatively, the photon beams used in this work could be replaced with proton shoot-through techniques: Similar planning geometries with comparable OAR sparing might be possible by utilizing the sharp penumbra of transmission beams.[49] At the same time, they could enable the introduction of range verification[50] and use of the FLASH effect.[51] Yet, the advantage of the much larger availability of photons may support effective LET-shaping for a larger group of patients by potentially reducing the number of required proton fractions or treatment time compared to mono-modal proton approaches at similar quality of the LET-distributions. Such comprehensive comparisons may be the focus of future studies.

Future works may investigate an efficient method to navigate the described trade-off between LET management and cost to conformity. Furthermore, in the future, the use of LMOs in combined treatments using heavier ions such as helium and carbon can be explored. Unlike proton therapy, these modalities exhibit greater variations in LET and RBE in the case of heavier ions used in radiotherapy. Furthermore, heavier ions have sharper Bragg peaks, enabling highly conformal dose distributions. While overdosing LMOs may show a more limited use, they could be particularly valuable for complex geometries or difficult beam arrangements. That said, objectives that focus on increasing and homogenizing LET and *dirty dose* in the target area can have a similar effect to those used in multi-ion therapy approaches.[17]

5 | CONCLUSION

This study demonstrates the feasibility and potential of incorporating LET-based objective functions into jointly optimized proton–photon treatment plans. By leveraging the complementary physical and biological properties of each modality, these strategies manage a trade-off

between dose conformity and high-LET delivered in critical structures, enabling safer and potentially more effective radiation therapy.

Both optimization of dose-weighted LET and *dirty dose* proved effective, with the *dirty dose* objective demonstrating more intuitive LET-painting capabilities in the joint setting, especially when adding target LET prescriptions.

The observed improvements in target coverage and OAR sparing emphasize the potential of LET-based mixed-modality optimization to extend the repertoire of precise radiation therapy. These results point to a promising path for the development of biologically guided planning strategies that improve both the safety and efficiency of particle therapy using existing treatment resources.

ACKNOWLEDGMENTS

This work was, in part, funded by the Deutsche Forschungsgemeinschaft (DFG, German Research Foundation)—Project No. 443188743.

Open access funding enabled and organized by Projekt DEAL.

CONFLICT OF INTEREST STATEMENT

The authors declare no conflicts of interest.

REFERENCES

1. Rorvik E, Fjera LF, Dahle TJ, et al. Exploration and application of phenomenological RBE models for proton therapy. *Phys Med Biol*. 2018;63(18):185013. doi:10.1088/1361-6560/aad9db
2. McNamara AL, Schuemann J, Paganetti H. A phenomenological relative biological effectiveness (RBE) model for proton therapy based on all published in vitro cell survival data. *Phys Med Biol*. 2015;60(21):8399. doi:10.1088/0031-9155/60/21/8399
3. Paganetti H, Blakely E, Carabe-Fernandez A, et al. Report of the AAPM TG-256 on the relative biological effectiveness of proton beams in radiation therapy. *Med Phys*. 2019;46(3):e53-e78. doi:10.1002/mp.13390
4. Ödén J, Toma-Dasu I, Witt Nyström P, Traneus E, Dasu A. Spatial correlation of linear energy transfer and relative biological effectiveness with suspected treatment-related toxicities following proton therapy for intracranial tumors. *Med Phys*. 2020;47(2):342-351. doi:10.1002/mp.13911
5. Henjum H, Dahle TJ, Fjæra LF, et al. The organ sparing potential of different biological optimization strategies in proton therapy. *Adv Radiat Oncol*. 2021;6(6):100776. doi:10.1016/j.adro.2021.100776
6. Giovannini G, Böhlen T, Cabal G, et al. Variable RBE in proton therapy: comparison of different model predictions and their influence on clinical-like scenarios. *Radiat Oncol*. 2016;11(1):68. doi:10.1186/s13014-016-0642-6
7. Giantsoudi D, Grassberger C, Craft D, Niemierko A, Trofimov A, Paganetti H. Linear energy transfer-guided optimization in intensity modulated proton therapy: feasibility study and clinical potential. *Int J Radiat Oncol Biol Phys*. 2013;87(1):216-222. doi:10.1016/j.ijrobp.2013.05.013
8. Deng W, Yang Y, Liu C, et al. A critical review of LET-based intensity-modulated proton therapy plan evaluation and optimization for head and neck cancer management. *Int J Particle Ther*. 2021;8(1):36-49. doi:10.14338/IJPT-20-00049.1
9. McIntyre M, Wilson P, Gorayski P, Bezak E. A systematic review of LET-guided treatment plan optimisation in proton therapy: identifying the current state and future needs. *Cancers*. 2023;15(17):4268. doi:10.3390/cancers15174268
10. Grün R, Friedrich T, Traneus E, Scholz M. Is the dose-averaged LET a reliable predictor for the relative biological effectiveness? *Med Phys*. 2019;46(2):1064-1074. doi:10.1002/mp.13347
11. McMahon SJ, Paganetti H, Prise KM. LET-weighted doses effectively reduce biological variability in proton radiotherapy planning. *Phys Med Biol*. 2018;63(22):225009. doi:10.1088/1361-6560/aae8a5
12. Liu C, Patel SH, Shan J, et al. Robust optimization for intensity modulated proton therapy to redistribute high linear energy transfer from nearby critical organs to tumors in head and neck cancer. *Int J Radiat Oncol Biol Phys*. 2020;107(1):181-193. doi:10.1016/j.ijrobp.2020.01.013
13. Cao W, Khabazian A, Yepes PP, et al. Linear energy transfer incorporated intensity modulated proton therapy optimization. *Phys Med Biol*. 2017;63(1):015013. doi:10.1088/1361-6560/aa9a2e
14. Unkelbach J, Botas P, Giantsoudi D, Gorissen BL, Paganetti H. Reoptimization of intensity modulated proton therapy plans based on linear energy transfer. *Int J Radiat Oncol Biol Phys*. 2016;96(5):1097-1106. doi:10.1016/j.ijrobp.2016.08.038
15. Traneus E, Ödén J. Introducing proton track-end objectives in intensity modulated proton therapy optimization to reduce linear energy transfer and relative biological effectiveness in critical structures. *Int J Radiat Oncol Biol Phys*. 2019;103(3):747-757. doi:10.1016/j.ijrobp.2018.10.031
16. Bassler N, Toftegaard J, Lühr A, et al. LET-painting increases tumour control probability in hypoxic tumours. *Acta Oncologica*. 2014;53(1):25-32. doi:10.3109/0284186X.2013.832835
17. Kopp B, Mein S, Dokic I, et al. Development and validation of single field multi-ion particle therapy treatments. *Int J Radiat Oncol Biol Phys*. 2020;106(1):194–205. doi:10.1016/j.ijrobp.2019.10.008
18. Unkelbach J, Fabiano S, Bennan ABA, Mueller S, Bangert M. Joint optimization of radiotherapy treatments involving multiple radiation modalities. *IEEE Trans Radiat Plasma Med Sci*. 2021;6(3):294-303, doi:10.1109/TRPMS.2021.3092423
19. Bennan ABA, Unkelbach J, Wahl N, Salome P, Bangert M. Joint optimization of photon–carbon ion treatments for Glioblastoma. *Int J Radiat Oncol Biol Phys*. 2021;111(2):559-572. doi:10.1016/j.ijrobp.2021.05.126
20. Fabiano S, Balermpas P, Guckenberger M, Unkelbach J. Combined proton–photon treatments – a new approach to proton therapy without a gantry. *Radiother Oncol*. 2020;145:81-87. doi:10.1016/j.radonc.2019.12.013
21. Fabiano S, Bangert M, Guckenberger M, Unkelbach J. Accounting for range uncertainties in the optimization of combined proton-photon treatments via stochastic optimization. *Int J Radiat Oncol Biol Phys*. 2020;108:792-801. doi:10.1016/j.ijrobp.2020.04.029
22. Unkelbach J, Bangert M, De Amorim Bernstein K, Andratschke N, Guckenberger M. Optimization of combined proton–photon treatments. *Radiother Oncol*. 2018;128(1):133-138. doi:10.1016/j.radonc.2017.12.031
23. Torelli N, Bicker Y, Marc L, Fabiano S, Unkelbach J. A new approach to combined proton-photon therapy for metastatic cancer patients. *Phys Med Biol*. 2024;69(14):145008. doi:10.1088/1361-6560/ad5d48
24. Marc L, Fabiano S, Wahl N, Linsenmeier C, Lomax AJ, Unkelbach J. Combined proton-photon treatment for breast cancer. *Phys Med Biol*. 2021;66(23):235002. doi:10.1088/1361-6560/ac36a3
25. Bennan ABA. Combined photon-carbon ion radiotherapy treatment planning. Dissertation. heiDOK. 2022. doi:10.11588/heidok.00030888
26. Papp D, Unkelbach J. Technical note: optimal allocation of limited proton therapy resources using model-based patient selection. *Med Phys*. 2022;49:4980-4987. doi:10.1002/mp.15812

27. Fredriksson A, Glimelius L, Bokrantz R. The LET trilemma: conflicts between robust target coverage, uniform dose, and dose-averaged LET in carbon therapy. *Med Phys*. 2023;50:7338-7348. doi:10.1002/mp.16771
28. Heuchel L, Hahn C, Ödén J, et al. The dirty and clean dose concept: towards creating proton therapy treatment plans with a photon-like dose response. *Med Phys*. 2024;51(1):622-636. doi:10.1002/mp.16809
29. McMahon SJ. The linear quadratic model: usage, interpretation and challenges. *Phys Med Biol*. 2018;64:24. doi:10.1088/1361-6560/aaf26a
30. AAPM. AAPM TG119 Dataset. Zenodo. 2023. doi:10.5281/zenodo.8037934
31. Wieser HP, Cisternas E, Wahl N, et al. Development of the open-source dose calculation and optimization toolkit matRad. *Med Phys*. 2017;44(6):2556-2568. doi:10.1002/mp.12251
32. Wieser HP, Wahl N, Gabryś HS, et al. matRad - an open-source treatment planning toolkit for educational purposes. *Med Phys Int*. 2018;6(1):119-127.
33. Ackermann B, Bangert M, Bennan ABA, et al. e0404/matRad: Blaise v2.10.0. Zenodo. 2020. doi:10.5281/zenodo.3879616
34. Wachter A, Biegler LT. On the Implementation of a Primal-Dual Interior Point Filter Line Search Algorithm for Large-Scale Nonlinear Programming. *Math Program*. 2005;106(1):25-57. doi:10.1007/s10107-004-0559-y
35. Shusharina N, Bortfeld T, Cardenas C, et al. Cross-modality brain structures image segmentation for the radiotherapy target definition and plan optimization. In: Shusharina N, Heinrich MP, Huang R., eds. *Segmentation, Classification, and Registration of Multi-Modality Medical Imaging Data*. Vol 12587. Springer International Publishing; 2021:3-15.
36. Combs SE, Kieser M, Rieken S, et al. Randomized phase II study evaluating a carbon ion boost applied after combined radiochemotherapy with temozolomide versus a proton boost after radiochemotherapy with temozolomide in patients with primary glioblastoma: the CLEOPATRA Trial. *BMC Cancer*. 2010;10(1):478. doi:10.1186/1471-2407-10-478
37. QI XS, Schultz CJ, Li XA. An estimation of radiobiologic parameters from clinical outcomes for radiation treatment planning of brain tumor. *Int J Radiat Oncol Biol Phys*. 2006;64(5):1570-1580. doi:10.1016/j.ijrobp.2005.12.022
38. Malaise EP, Fertil B, Deschavanne PJ, Chavaudra N, Brock WA. Initial slope of radiation survival curves is characteristic of the origin of primary and established cultures of human tumor cells and fibroblasts. *Radiat Res*. 1987;111(2):319-333. doi:10.2307/3576988
39. Wigg DR. Applied radiobiology and bioeffect planning. *Australas Phys Eng Sci Med*. 2002;25(1):44.
40. Schultz CT, Geard CR. Radioresponse of human astrocytic tumors across grade as a function of acute and chronic irradiation. *Int J Radiat Oncol Biol Phys*. 1990;19(6):1397-1403. doi:10.1016/0360-3016(90)90350-S
41. Murshed H. *Fundamentals of Radiation Oncology: Physical, Biological, and Clinical Aspects*. 3rd ed. Elsevier Science & Technology; 2019.
42. Krämer M, Scifoni E, Schmitz F, Sokol O, Durante M. Overview of recent advances in treatment planning for ion beam radiotherapy. *Eur Phys J D*. 2014;68(10):306. doi:10.1140/epjd/e2014-40843-x
43. Bahn E, Bauer J, Harrabi S, Herfarth K, Debus J, Alber M. Late contrast enhancing brain lesions in proton-treated patients with low-grade glioma: clinical evidence for increased periventricular sensitivity and variable RBE. *Int J Radiat Oncol Biol Phys*. 2020;107:571-578. doi:10.1016/j.ijrobp.2020.03.013
44. Eulitz J, Troost EGC, Klünder L, et al. Increased relative biological effectiveness and periventricular radiosensitivity in proton therapy of glioma patients. *Radiother Oncol*. 2023;178:109422. doi:10.1016/j.radonc.2022.11.011
45. Palkowtisch M, Kaufmann LM, Hennings F, et al. Variable-RBE-induced NTCP predictions for various side-effects following proton therapy for brain tumors – identification of high-risk patients and risk mitigation. *Radiother Oncol*. 2025;202:110590. doi:10.1016/j.radonc.2024.110590
46. Amstutz F, Krcek R, Bachtiary B, et al. Treatment planning comparison for head and neck cancer between photon, proton, and combined proton–photon therapy – from a fixed beam line to an arc. *Radiother Oncol*. 2024;190:109973. doi:10.1016/j.radonc.2023.109973
47. Bertolet A, Carabe A. Proton monoenergetic arc therapy (PMAT) to enhance LETd within the target. *Phys Med Biol*. 2020;65(16):165006. doi:10.1088/1361-6560/ab9455
48. Toussaint L, Indelicato DJ, Holgersen KS, et al. Towards proton arc therapy: physical and biologically equivalent doses with increasing number of beams in pediatric brain irradiation. *Acta Oncologica*. 2019;58(10):1451-1456. doi:10.1080/0284186X.2019.1639823
49. Kong W, Huiskes M, Habraken SJM, et al. Reducing the lateral dose penumbra in IMPT by incorporating transmission pencil beams. *Radiother Oncol*. 2024;198:110388. doi:10.1016/j.radonc.2024.110388
50. Engwall E, Mikhalev V, Sundström J, Marthin O, Wase V. Shoot-through layers in upright proton arcs unlock advantages in plan quality and range verification. *Med Phys*. 2025;52:e18051. doi:10.1002/mp.18051
51. Verhaegen F, Wanders RG, Wolfs C, Eekers D. Considerations for shoot-through FLASH proton therapy. *Phys Med Biol*. 2022;66:06NT01. doi:10.1088/1361-6560/abe55a

SUPPORTING INFORMATION

Additional supporting information can be found online in the Supporting Information section at the end of this article.

How to cite this article: Seckler L, Bennan ABA, Wahl N. Impact of LET-modifying planning objectives on the optimization of mixed-modality proton–photon treatments. *Med Phys*. 2026;53:e70478. https://doi.org/10.1002/mp.70478